RSC Advances

PAPER

View Article Online
View Journal | View Issue

Cite this: *RSC Adv.*, 2021, **11**, 4174

A SnO_2 shell for high environmental stability of Ag nanowires applied for thermal management†

Anna Baranowska-Korczyc, *[a] Ewelina Mackiewicz, [a] Katarzyna Ranoszek-Soliwoda, [a] Alicja Nejman, [b] Susana Trasobares, [c] Jarosław Grobelny, [a] Małgorzata Cieślak [b] and Grzegorz Celichowski *[a]

Since silver nanowires (AgNWs) show high infrared reflectance many studies present their applicability as thermal management products for various wearable textiles. However, their use for practical purposes is only partially evaluated, without focusing on improving their low atmospheric and liquid stability. This report describes a new approach for the topic and proposes a facile method of Ag nanowire passivation with a SnO_2 layer for high environmental stability and retention of high infrared reflectance. The one-step passivation process of AgNWs was carried out in the presence of sodium stannate in an aqueous solution at 100 °C, and resulted in the formation of core/shell Ag/SnO_2 nanowires. This study presents the morphological, chemical, and structural properties of Ag/SnO_2NWs formed with a 14 nm thick SnO_2 shell, consisting of 7 nm rutile-type crystals, covering the silver metallic core. The optical properties of the AgNWs changed significantly after shell formation, and the longitudinal and transverse modes in the surface plasmon resonance spectrum were red shifted as a result of the surrounding media dielectric constant changes. The passivation process protected the AgNWs from decomposition in air for over 4 months, and from dissolution in a KCN solution at concentrations up to 0.1 wt%. Moreover, the report shows the microwave irradiation effect on the shell synthesis and previously synthesised Ag/SnO_2NWs. The post-synthesis irradiation, as well as the SnO_2 shell obtained by microwave assistance, did not allow long-term stability to be achieved. The microwave-assisted synthesis process was also not fast enough to inhibit the formation of prismatic silver structures from the nanowires. The Ag/SnO_2NWs with a shell obtained by a simple hydrolysis process, apart from showing high infra-red reflectance on the *para*-aramid fabric, are highly environmentally stable. The presented SnO_2 shell preparation method can protect the AgNW's surface from dissolution or decomposition and facilitate the designing of durable smart wearable thermal materials for various conditions.

Received 27th November 2020
Accepted 14th January 2021

DOI: 10.1039/d0ra10040d

rsc.li/rsc-advances

Introduction

Silver nanowires (AgNWs) have attracted increasing attention in optoelectronics, sensing and energy-saving applications due to their high electrical conductivity, high transmittance, excellent plasmonic properties, infrared radiation reflectivity, nanometric size and quasi-one dimensional (1D) geometry.[1] Their use as basic building blocks in a wide range of nanodevices and materials has been extensively considered.[2] Recently, the concept of "personal thermal management" based on silver nanowires, has been particularly highlighted and initiated for the design of various textiles.[3,4] Due to the AgNWs' ability to reflect human body infrared radiation and reduce heat loss, they are applied in creating smart wearable materials.[5,6] However, AgNWs use for practical purposes is limited by their low chemical and thermal stability, low adhesion, electrical instabilities, and ageing processes.[7] Although the number of reports investigating AgNWs as a material for thermal management is steadily growing, these still represent only a partial evaluation of the topic, without focusing on nanowires stability. The main concerns about the silver nanostructures applications are focussed on the fact that they corrode at ambient conditions. Atmospheric corrosion of silver nanowires covered with PVP, as a commonly used capping agent during the polyol synthesis process, has been extensively studied by Elechiguerra *et al.*[8] They found that the polymer layer is permeable to gases and water vapour and does not inhibit atmospheric corrosion of the NWs due to the high reactivity of nanoscale silver and the presence of defects along the

[a]*The University of Lodz, Faculty of Chemistry, Department of Materials Technology and Chemistry, Pomorska 163, 90-236 Lodz, Poland. E-mail: grzegorz.celichowski@chemia.uni.lodz.pl; anna.korczyc@chemia.uni.lodz.pl*

[b]*LUKASIEWICZ–Textile Research Institute, Department of Chemical Textiles Technologies, 5/15 Brzezinska Street, 92-103 Lodz, Poland*

[c]*Department of Materials Science and Metallurgical Engineering and Inorganic Chemistry, University of Cadiz, 11003 Cadiz, Spain*

† Electronic supplementary information (ESI) available. See DOI: 10.1039/d0ra10040d

nanowires. In an aquatic environment, AgNWs also reveal low stability because they are influenced by two processes: dissolution and sulphidation.[9] The dissolution leads to the decomposition of the initial nanowire to shorter structures like rods, and additionally, extends their surface area for further corrosion. Sulphidation is one of the most important processes on silver nanomaterial surfaces due to the effective interaction of Ag^+ ions with reduced-sulphur gases, which results in the formation of a thin, non-conductive, silver sulphide layer.[8] Moreover, Ag_2O and AgO can also be formed as a consequence of local oxidation of the silver nanostructure surface.[10]

To enhance the AgNWs processability and avoid chemical instability, which does not facilitate their integration in future devices and textiles, various approaches have been applied after the synthesis process. One of the ideas is thermal annealing and electrical welding to minimise the junction resistance between single nanostructures in the AgNWs network. However, due to the high surface area to volume ratio of nanowires, in comparison to the bulk material, high temperature above 300 °C can cause melting or spheroidisation of AgNWs and the loss of percolation pathways.[7] The chemical stability of Ag nanostructures can be improved by forming an alloy with more stable metals such as Au. The synthesis of this kind of alloy is complicated due to significant differences in both the component reactivity and reducing their precursors at the same time.[11] A facile and effective method to inhibit silver nanostructure corrosion is the synthesis of a protective coating layer which results in the formation of core/shell alignment. The silver nanowires have been previously covered with titanium dioxide (TiO_2) and their thermal stability increased to 750 °C due to the suppression of silver atom motion at the Ag/TiO_2 interface.[12] A significant enhancement of adhesion as well as thermal and electrical stability of AgNWs, with only a small decrease in optical transparency, was obtained by forming a zinc oxide (ZnO) coating on Ag nanostructures.[7] On the other hand, ZnO is known as a compound with low stability in an aquatic environment, especially at the nanoscale.[13]

One of the promising non-organic coating material is tin oxide (SnO_2), which shows high mechanical, thermal, and chemical stability and can be applied as a protective shell for silver nanostructures.[14–16] AgNWs were decorated with SnO_2 nanoparticles to obtain thermal stability and to minimise the annealing procedures and post-treatment of silver nanowires.[17] SnO_2 layer, as an anti-corrosion coating for Ag nanowires protection, has been previously presented only in the form of a monolayer, which was grown in solution overnight under the treatment of stannous fluoride (SnF_2), additionally covered with amorphous carbon layer.[18]

This study presents a rapid method of SnO_2 shell formation on AgNWs. The obtained SnO_2 shell improves the Ag nanowires stability in the air, or even in strongly complexing solutions such as cyanides, as well as providing long-term stability. The SnO_2 layer on the AgNWs surface was formed in a one-step synthesis process by the treatment of sodium stannate in aqueous solution. The SnO_2 shell is characterised by a thickness of 14 nm and formed by 7 nm rutile-type crystals. The characterisation of the core/shell Ag/SnO_2NWs was performed using STEM (Scanning Transmission Electron Microscopy), TEM (Transmission Electron Microscopy), EELS (Electron Energy Loss Spectroscopy), UV/Vis, and XPS (X-ray Photoelectron Spectroscopy) analysis. The high efficiency of the SnO_2 shell was proven in ambient conditions and in a harsh KCN environment (up to 0.1 wt%), and by long-term stability for over four months. Moreover, Ag/SnO_2NWs were applied on a *para*-aramid textile to show that silver nanowire infrared reflectance properties are maintained. The thermal properties of the *para*-aramid with deposited nanowires were studied using the Alambeta tests, DSC (Differential Scanning Calorimetry) and TG/DTG (Thermogravimetry/Derivative Thermogravimetry) analysis. The proposed system might find applications in fabrics designed for saving energy and maintaining warmth in the human body under different environmental conditions.

Experimental details

Synthesis of AgNWs

A mixture of 40 ml of ethylene glycol (EG, POCH), 2 g of polyvinyl pyrrolidone (PVP, molecular weight of 55 kDa, Sigma Aldrich) and 0.028 g of sodium chloride (NaCl, Chempur) was heated to 170 °C and stirred at 570 rpm to obtain a homogenous solution. Then, a mixture of 0.408 g previously dissolved $AgNO_3$ (purity 99.9999%, Sigma-Aldrich) in 20 ml of EG was added, dropwise, to the constantly heated, refluxed and stirred solution of EG, PVP and NaCl. The feed rate was 16 ml h^{-1}. After delivering the whole amount of $AgNO_3$, the solution was kept at the above-described conditions for 1 h and then air-cooled to room temperature. In order to remove PVP from the solution, it was diluted by acetone in the ratio of 1 : 10, and then the AgNWs were dispersed in 60 ml of ethanol (anhydrous, POCH).

SnO_2 shell formation on AgNWs under high temperature

For a typical shell synthesis, 2.5 g of AgNWs solution was added to 92.7 g of deionised water (Deioniser Millipore Simplicity System) and mixed with 4.78 g of a 1 wt%. aqueous solution of sodium citrate ($Na_3C_6H_5O_7 \cdot 2H_2O$, purity 99.0%, Sigma Aldrich). The solution was heated to water boiling point (100 °C) under reflux with 300 rpm continuous stirring. Then, 5.051 g of a 0.25 wt%. aqueous solution of sodium stannate trihydrate ($Na_2SnO_3 \cdot 3H_2O$, Sigma-Aldrich, 95%) was added to the silver nanowires mixture at 100 °C and the mixture was maintained at the same conditions for the next 15 min. Then the mixture was cooled in cold water bath.

SnO_2 shell formation on AgNWs under high-temperature and microwave irradiation

In microwave-assisted shell synthesis, 2.5 g of AgNWs solution was added to 92.7 g of deionised water, 4.78 g of a 1 wt% aqueous solution of sodium citrate and 5.051 g of a 0.25 wt% aqueous solution of sodium stannate trihydrate. The mixture was irradiated by microwave at 150 °C for 30 minutes under magnetic stirring (Microwave Reaction System, Anthon Paar GmbH – Synthos 3000). During the irradiation process, the power increased with heating temperature increasing but not

exceed 250 Watt (the maximum power) and pressure of 100 PSI. The applied temperature and synthesis time were optimised to achieve the conditions of 100 °C for at least 15 minutes in the sample chamber for comparison with the shell obtained without microwave assistance.

Moreover, core/shell Ag/SnO_2NWs prepared without microwave treatment (aqueous solution) were irradiated after the synthesis by microwave at 150 °C, a pressure of 100 PSI, maximum power of 250 Watt and time of 30 min under magnetic stirring.

Characterisation and stability studies of core/shell Ag/SnO_2NWs

The morphology and size of Ag and core/shell Ag/SnO_2 nanowires were determined using the STEM imaging capacity at the SEM microscope (microscope NovaNanoSEM 450 FEI equipped with STEM II detector for transmitted electron detection, an accelerating voltage of 30 kV). The optical properties of the NWs were determined using UV/Vis spectroscopy (Spectrophotometer UV5600, Biosens) at the wavelength range of 190 to 1100 nm. The stability of the AgNWs coated with an SnO_2 layer under high temperature and/or microwave treatment, was studied using STEM imaging within several weeks at ambient condition. The samples after the synthesis were put on copper grids (300 mesh) with a carbon support layer, stored in air at room temperature, and measured every few days.

Moreover, the core/shell Ag/SnO_2NWs were treated with an aqueous solution of KCN at different concentrations of 0.0001, 0.001, 0.01 and 0.1 wt%. To study the influence of the SnO_2 shells, obtained with and without the assistance of microwave irradiation, on the AgNWs chemical stability in the strongly complexing solution of CN^-, their optical properties were evaluated using absorbance measurements in the wavelength range of 190 to 1100 nm.

The structural characterisation of the selected core/shell Ag/SnO_2 nanowires characterised by high environmental stability (Ag/SnO_2NWs synthesised without microwave irradiation assistance) was performed using TEM and EELS analysis (JEOL 2010F operating at 200 kV, equipped with a HAADF detector, an EELS spectrometer GIF2000 Gatan Imaging Filter). The EELS spectra were recorded using the spectrum imaging (SI) modes. The SI mode consists on acquiring a simultaneously HAADF signal and a collection of spectra at successive positions while the fine electron probe (0.5 nm in our experiments) is scanned over a predefined region in the sample. This approach allows correlating nanoanalytical and structural information of the region under study. EELS spectra with 0.3 eV energy dispersion, aperture of 5 mm and speed of 0.1 s per spectrum were recorded with convergence and collection semiangles of 8 and 24 mrad. XPS analysis was applied to evaluate the surface elemental composition of the core/shell system. The Ag/SnO_2NWs were deposited on a silicon wafer coated with 100 nm of gold. An X-ray photoelectron spectrometer (Axis Supra, Kratos Analytical) with a monochromatic X-ray beam (energy of 1486.6 eV) was used for the study. The photoemission spectra were collected in a wide range of binding energies from −5 to 1200 eV.

Preparation and characterisation of Ag/SnO_2NWs *para*-aramid composite fabric

The *para*-aramid, poly(1,4-terephthalate-fenylodiamid) fabric made of doubled, staple 20 × 2 tex yarn, Kevlar® (DuPont, London, United Kingdom) with a surface mass of 165 g m^{-2} was cut into 50 × 50 mm pieces and ultrasonic spray-coated (105 kHz) with 1 ml of aqueous solutions of AgNWs and Ag/SnO_2-NWs. The both solutions were centrifuged (8000 rpm, 5 minutes) and re-suspended to obtain a concentration of 7000 ppm of silver. The solutions before spray-coating process were homogenized (120 Watt, Hielscher homogenizer: model U200S) for 3 minutes.

The heat transfer analysis of AgNWs and Ag/SnO_2NWs spray-coated and uncoated (control sample) fabrics were performed on Alambeta (Sensora, Czech Republic) apparatus. The Alambeta tests[19] were based on measuring the amount of heat flowing through the sample placed between two plates – the upper one, heated up to about 32 °C and the bottom one with a temperature of 22 °C. The plates of 110 cm^2 area exerted a constant pressure of 200 Pa ± 10%. Measurements were taken at the temperature of 20 °C and relative humidity of 27% for 5 minutes.

The thermal properties of uncoated (control sample) and spray-coated *para*-aramid fabric with AgNWs and Ag/SnO_2NWs were studied using DSC. The measurements were carried out using the differential scanning calorimeter DSC 204 F1 Phoenix (Netzsch, Germany). The samples with a weight of about 4 mg were placed in a ceramic crucible with a volume of 85 μl and heated in the temperature range of 20–600 °C with a rate of 10 °C min^{-1} under nitrogen (gas flow 25 ml min^{-1}). TG/DTG analysis of the pure fabric, which acted as a control sample and fabric with deposited AgNWs and Ag/SnO_2NWs as well as powders of AgNWs, and Ag/SnO_2NWs was performed on thermogravimetry analyzer TG 209F1 Libra (Netzsch, Germany). The samples with a weight of about 2–4 mg were placed in a ceramic crucible with a volume of 85 μl. The measurements were carried out in the temperature range of 20–800 °C with a heating rate of 10 °C min^{-1} under a nitrogen flow rate of 25 ml min^{-1}.

Infrared thermography studies of the *para*-aramid fabric before and after the modification processes were performed with a thermal imaging camera VarioCAM (InfraTec., Germany), recording thermograms in the form of a colour image with a resolution of 640 × 480 pixels. The camera was equipped with an uncooled, microbolometer detector with a spectral range of 8–13 μm. The samples were placed on a heating plate in which temperature was regulated in the range of 35 to 40 °C, in 1 °C steps. The distance of the camera from the plate surface was 1 m. Measurements were made at 23.4 °C and RH = 75 ± 2%. For each test, 20 thermograms were made, being recorded every 1 s. Processing and analysis of the obtained thermograms were performed using the IRBIS V2.2 software.

Results and discussion

In this study, AgNWs were obtained by the polyol method, optimised in our previous reports.[21,22] AgNWs were

characterised by a mean diameter of 42 (±3) nm (Fig. S1(a)†) and the average length of 7.6 (±1.7) μm. The size of the nanowires was estimated based on STEM measurement of about 100 single nanostructures. The stability of the AgNWs was studied in ambient conditions, in the air at room temperature over several weeks using STEM imaging (Fig. S2†). The stability of the silver nanowires in the air is known to be low due to relatively fast silver surface corrosion and the decomposition process.[8] The morphology of the AgNWs changed after just one week during constant exposure to air (Fig. S2(b)†). The nanowire surface was no longer smooth and revealed visible clusters, which were not homogeneously distributed along the silver nanostructures. The corrosion process does not have the same rate in different regions of the same nanowire. The surface defect accumulation and local lower surface coverage with PVP coating promote the corrosion and higher rate of the process.[8] The number of inclusions on the nanowires increased with time, after 2, 3, 7, and 9 weeks, resulting in the decomposition of the nanostructures (Fig. S2†). The atmospheric corrosion of silver nanostructures is caused mainly by the sulphidation process and not, as might be predicted, by the oxidation process.[23] Hydrogen sulphide (H_2S) and carbonyl sulphide (OCS) have been shown to be the most important corrodent agents for the tarnishing and decomposition process of silver materials in the air, about one order of magnitude higher than the rates for other sulphur gases, such as sulphur dioxide (SO_2) and carbon disulphide (CS_2).[23] It was found that H_2S at a concentration of 0.2 ppb in the air is sufficient to initiate a silver corrosion process and form a crystalline form of silver sulphide (Ag_2S).[24] Carbonyl sulphide also significantly influences the silver surface by relatively fast decomposition into H_2S.

To improve the chemical stability of the silver surface, the nanowires were passivated with a tin oxide layer. The synthesis of the SnO_2 shell was carried out by two methods, the first of which was stannate hydrolysis (according to eqn (1)–(4)), previously presented in our report on AgNPs.[16] The process is achievable at a temperature above 60 °C in aqueous solution; in this study the synthesis was carried out at 100 °C (Fig. 1(a), S1(b) and S3(a)†). The second technique was also a stannate hydrolysis process in aqueous solution, but under a combination of high temperature and microwave irradiation (Fig. 1(b) and S3(b)†). The microwave irradiation was applied for shell synthesis as a factor previously used in many reports for SnO_2 growth.[25,26] The comparison of the environmental stability of both samples enabled the further sample selection, characterised by high resistance to atmospheric conditions and chemicals.

$$Na_2SnO_3 + 2H_2O \rightarrow H_2SnO_3\downarrow + 2NaOH \quad (1)$$

$$SnO_3^{2-} + 3H_2O \rightarrow Sn(OH)_4\downarrow + 2OH^- \quad (2)$$

$$Sn(OH)_4 + 2OH^- \rightarrow Sn(OH)_6^{2-} \quad (3)$$

$$Sn(OH)_6^{2-} \rightarrow SnO_2\downarrow + 2OH^- + 2H_2O \quad (4)$$

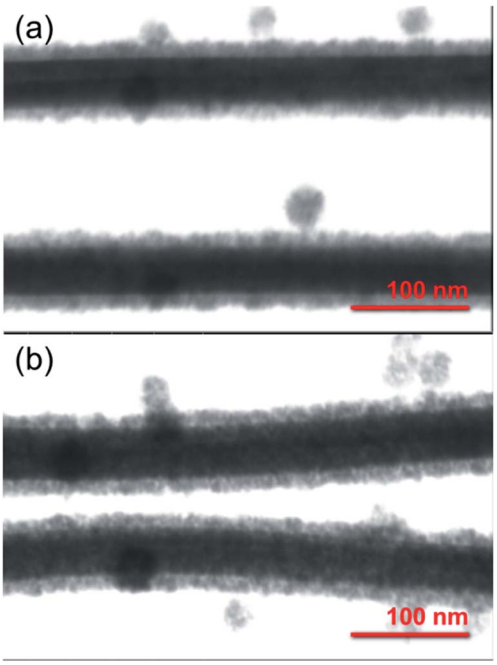

Fig. 1 STEM images of core/shell Ag/SnO_2NWs. The SnO_2 shell was obtained (a) without and (b) with microwave irradiation assistance.

The core/shell Ag/SnO_2 nanostructure synthesis can prevent diffusion of Ag atoms and structural damage, as well as enhance their chemical stability. STEM images of the Ag/SnO_2NWs (Fig. 1) obtained by both methods revealed uniform coatings on the nanowires along the whole silver structures. The thickness of the shell was about 14 nm (±2 nm) for both applied techniques (Fig. 1). However, microwave irradiation affected the AgNWs during the synthesis of the SnO_2 coating. It caused the formation of silver particles and rods due to the fast decomposition process of the nanowires before the creation of the SnO_2 protecting layer (Fig. S3(b)†). The microwave treated AgNWs, without providing a substrate of sodium stannate caused the rearrangement of the nanowires into rods and particles (Fig. S4†). The sample irradiated with the presence of sodium stannate showed a mixture of nanowires, rods and particles, all covered with the SnO_2 shell. It indicates that a protective coating is formed for all silver nanostructures, but the process is not rapid enough to prevent the decomposition process from starting under microwave irradiation (Fig. 3S(b)†).

To get more insight into the SnO_2 shell synthesis process under microwave irradiation, the Ag/SnO_2NWs, obtained under high temperature only, were treated with microwaves after the coating synthesis. It was found that microwave irradiation did not influence the AgNWs morphology if they were previously coated with SnO_2 (Fig. S3(c)†).

The stability of the core/shell samples was studied for 4 months. The nanowires after the synthesis process were constantly exposed to the air and room temperature conditions for the whole studied time. The morphology of the Ag/SnO_2-NWs, for the shell obtained in aqueous solution under 100 °C, remained unchanged for 4 months (Fig. 2). The atmospheric

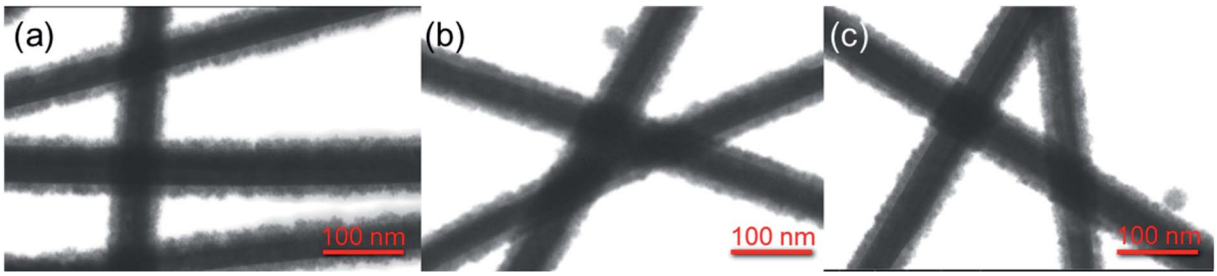

Fig. 2 STEM images of core/shell Ag/SnO_2NWs (a) after the synthesis, (b) after 3 weeks and (c) 4 months kept in air at room temperature. The SnO_2 shell was obtained without microwave irradiation assistance.

stability studies for AgNWs covered with SnO_2 under microwave irradiation (Fig. S5†) revealed an unaffected morphology of the wires after 3 weeks (Fig. S5b†), similar to Ag/SnO_2NWs, for which the shell was obtained without microwave assistance (Fig. 2(b)). The morphology of both samples showed stability for several weeks, but after a long time (several months) it differed significantly. After 4 months the silver core of the nanowires with the shell microwave treated had started to decompose in many places (indicated in Fig. S5(c)†), while Ag/SnO_2NWs non-microwave treated remained unchanged (Fig. 2(c)). The shell synthesised under microwave irradiation only protects the silver nanostructure to a certain extent, in comparison to the non-coated samples, which decomposed completely after 9 weeks of ambient condition exposure (Fig. S2†). This is not the long-term stability required for designing future devices and materials.

The studies also revealed the influence of microwave irradiation on the SnO_2 layer previously formed in aqueous solution at 100 °C. Although it prevents the formation of silver particles and rods as during the direct synthesis in microwaves, the microwave irradiation damaged the previously formed protective SnO_2 layer. The silver core decomposed after 5 weeks of laboratory ambient conditions (Fig. S6†). The impact of the applied microwave irradiation has been studied previously for the PdAgNW system.[27] The core/shell nanowires were synthesised by a microwave-assisted polyol method with pulse mode, however further microwave irradiation made the nanowires break into nanorods. Although the microwave-treated nanowires showed higher catalytic efficiency,[27] the microwave irradiation can have a harmful effect on the protective ability of the previously synthesised SnO_2 layer, or only form a short-term protective shell.

The optical properties of the core/shell Ag/SnO_2NWs also depend on the method of shell formation. The absorbance spectra of AgNWs show two major bands centred at around 349 nm and 376 nm (Fig. 3(a)). Their values are consistent with other reports and reveal, respectively, the plasmon response in the longitudinal and transverse modes of the AgNWs with five-fold symmetry.[28,29]

The AgNWs coated with SnO_2 under high temperature reveal a red shift for both major absorbance peaks. They were shifted to 361 nm and 415 nm for the longitudinal and transverse surface plasmon resonance modes of the silver nanowires, respectively (Fig. 3(b)). The plasmon response mode was red shifted to about 10 nm, whereas the transverse mode was shifted to about 40 nm. This indicates the effective formation of the coating on silver nanowires. The surface plasmon resonance (SPR) of silver nanowires is sensitive to the morphology and dielectric constant of the environment, which is significantly changed after coating the nanostructures. It was shown previously that the SPR modes of AgNWs covered with a TiO_2 shell revealed a gradual red shift upon the systematic build-up of the dielectric cover.[12]

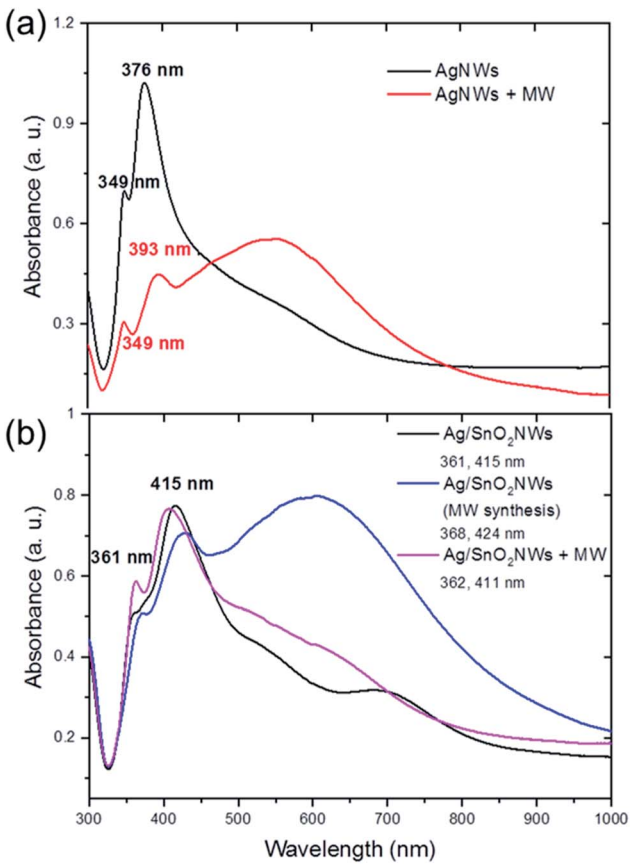

Fig. 3 Absorbance spectra of (a) as-synthesised and microwave treated AgNWs and (b) core/shell Ag/SnO_2NWs. (b) The SnO_2 shell was obtained without and with microwave irradiation assistance and was also treated with microwave irradiation after the shell synthesis process.

The two major bands for nanowires covered with the tin oxide layer obtained under simultaneous treatments of both high temperature and microwave irradiation are also comparable with core/shell samples synthesised without microwave treatment (Fig. 3(b)). The bands are centred at around 368 nm and 424 nm. However, a new band appears in the absorbance spectra with a maximum at around 620 nm, connected with the existence of new silver structures in the sample, prismatic triangular shape ones.[30,31] This is consistent with the results of the STEM observations, which show that microwave irradiation causes the formation of that shape of structures (Fig. S3(b)† inset). To study the influence of microwave irradiation on the optical properties of the as-synthesised AgNWs, their absorption was also measured. The spectra revealed that the maximum of the plasmon response longitudinal mode band remained unchanged while the maximum of the transverse mode was shifted to 393 nm (Fig. 3(a)). Moreover, a third wide band centred at around 545 nm appeared as a result of the silver cubes formation under microwave treatment, and the silver nanowires rearrangement.[30,32] In contrast to the microwave-assisted shell synthesis, in which triangular structures were formed, the as-synthesized AgNWs decompose mainly into cubical structures (see Fig. S4†). The shell synthesis with applied microwave assistance is not effective because it allows rearrangement of the silver material before the formation of the protective SnO_2 coating. However, the SnO_2 shell is formed on both AgNWs and silver prisms appearing in the sample under microwave irradiation.

The samples obtained under high-temperature treatment only did not improve, or even change, significantly, after post-synthesis microwave irradiation. The absorbance spectra did not change significantly after treating the core/shell Ag/SnO_2 nanowires with microwave irradiation (Fig. 2(b)). The main absorbance bands are centred at around 362 nm and 411 nm for the longitudinal and transverse modes of the nanowires, respectively. It indicates that the dielectric constant of the surrounding medium of silver nanowires did not change significantly.[33]

The SnO_2 shell obtained in both ways as well as improved by microwave irradiation was studied as a liquid stability improving factor. Since cyanides (CN^-) dissolve metals in the presence of oxygen they were selected for the stability studies. Cyanides are nucleophilic reagents, which can donate electrons to unoccupied orbitals on the coordinatively unsaturated surface of Ag nanostructures. Ag nanostructures are highly reactive toward oxygen, which allows atom complexation and dissolving in the form of $Ag(CN)_2^-$.[34] The complex is soluble and colourless and allows quantitative (absorbance intensity changes) and qualitative (colour loss) stability studies and verification of the protective effect of SnO_2 shell.

The core/shell Ag/SnO_2NWs and AgNWs samples were treated with KCN solution at a concentration of 0.0001 to 0.1 wt% as high complexing reagent (Fig. 4, S7 and S8†). The samples with the shell obtained by the hydrolysis process without microwave assistance shows two main absorbance bands at about 361 and 415 nm characteristic for the longitudinal and transverse modes of silver nanowires, respectively

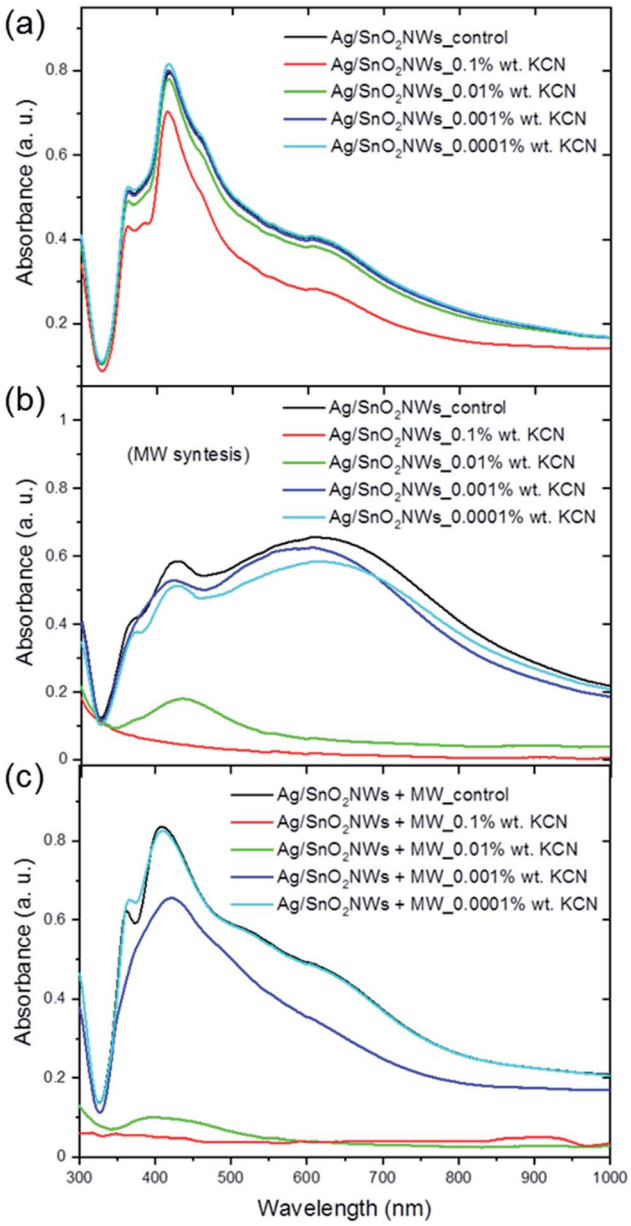

Fig. 4 Absorbance spectra of core/shell Ag/SnO_2NWs obtained (a) without and (b) with microwave irradiation assistance and (c) also treated with microwave irradiation after the shell synthesis process. The samples were treated with 0, 0.1, 0.01, 0.001, 0.0001 wt% KCN.

(Fig. 4(a)). The position of the bands remained unchanged in the entire concentration range of KCN. Moreover, only the CN^- ions at the highest concentration influenced, to some degree, the absorbance intensity of silver nanowires. The absorbance intensity of Ag/SnO_2NWs slightly decreased for 0.1 wt% KCN concentration. This indicates a high environmental stability of the proposed system as well as a high density and efficiency of the SnO_2 shell as an effective barrier layer which prevents the harmful influence of strong complexing CN^- ions on the silver nanowire core.

The core/shell Ag/SnO_2NWs with the shell obtained by a combination of the high temperature and microwave

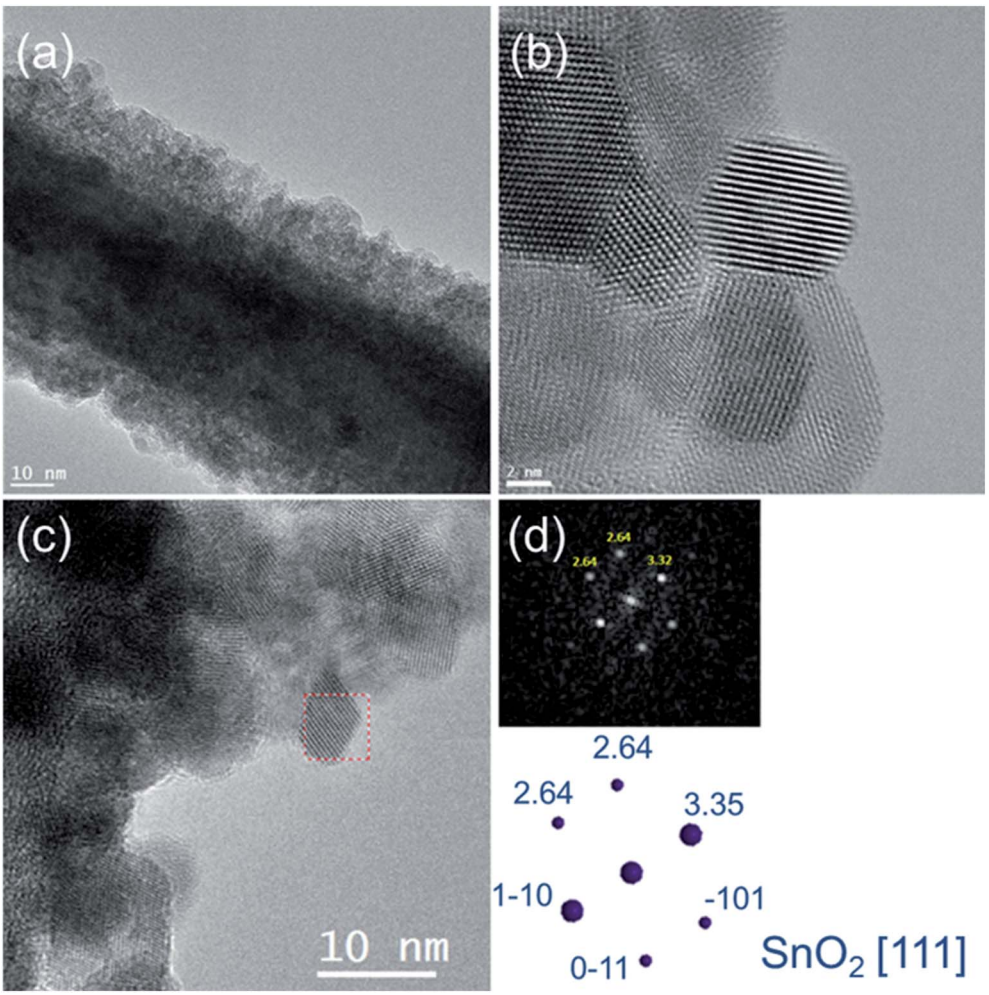

Fig. 5 (a) TEM and (b, c) HRTEM images of core/shell Ag/SnO_2NWs. (d) The electron diffraction pattern and (c) HRTEM image indicating the studied area of the SnO_2 shell.

irradiation was significantly influenced by the cyanides (Fig. 4(b)). For the highest concentration of the CN^- ions (0.1 wt%) the nanowires decomposed completely. For the concentration of 0.01 wt% only the peak at 415 nm characterised by low absorbance intensity is noted, which also indicates the decomposition and structural damage of the silver nanowires. The other concentrations also proportionally influenced the AgNWs absorbance intensity, which decreased for the two main silver nanowire bands and for the prismatic structures. The harmful influence of the CN^- ions is similar for the silver prismatic structures obtained by microwave irradiation because they were also only covered to the same extent with the SnO_2 shell during the stannate hydrolysis.

The images of the aqueous solution of Ag/SnO_2NWs treated with KCN (Fig. S7†) show the results consistent with the absorbance analysis. The colour of SnO_2/AgNWs samples characterised by the SnO_2 shell obtained at 100 °C remained unchanged for a wide applied range of KCN concentrations. The core/shell Ag/SnO_2NWs samples with the shell synthesised with microwave assistance changed colour significantly. They became colourless for KCN concentration of 0.1 and 0.01 wt%, indicating the decomposition of the nanowires.

The SnO_2 shell synthesised with microwave irradiation assistance did not show a protective effect for the applied concentration range of KCN. AgNWs were oxidised by dissolved oxygen in the presence of CN^- as a result of the redox reaction. The absorbance band intensity decreased due to the formation of a soluble and colourless complex of $Ag(CN)_2^-$.[35] This indicates that the shell synthesised with microwave assistance is permeable to cyanide ions and the crystallites inside the layer are not compressed enough to protect the core against environmental influences.

Moreover, the chemical stability of Ag/SnO_2NWs with the shell obtained by the hydrolysis process without microwave assistance, but irradiated with microwave after SnO_2 shell synthesis, was also studied (Fig. 4(c)). The samples revealed lower environmental stability against KCN in comparison to the non-irradiated ones (Fig. 4(a)), similar to those obtained with microwave treatment assistance (Fig. 4(b)). For the two highest concentrations of CN^- ions, the absorbance spectra did not show SPR bands typical for silver nanowires and the samples

became colourless as well (Fig. S7(c)†), indicating the decomposition of AgNWs. Only for the lowest concentration of cyanide ions of 0.0001 wt% did the absorbance spectrum and sample colour remain unchanged, similar to the as-synthesised AgNWs (Fig. S8†), showing that the concentration of CN^- ions was too low to affect the nanowires. The chemical stability studies of the core/shell Ag/SnO_2NWs sample treated with microwave after the shell synthesis revealed that irradiation damaged the protective effect of the SnO_2 shell. The microwave irradiation is a commonly used technique to obtain, or improve, the crystal structure of different ceramic nanomaterials, such as increasing the size of crystallites or changing the amorphous phase to a crystalline one at relatively low temperature.[36] It can result in the modification of the crystallite's alignment and compression within the SnO_2 layer, and these processes make it permeable to various environmental factors.

The atmospheric and liquid stability studies of the core/shell Ag/SnO_2NWs demonstrated that shell synthesis by simple hydrolysis at about 100 °C according to eqn (1)–(4) is the most effective and facile way to protect nanowires against environmental influence. Moreover, the shell synthesis without microwave assistance did not cause sample rearrangement and formation of other silver structures of different dimensionalities.

The structural properties of the most functional SnO_2 shell (synthesised without microwave irradiation assistance) were studied by TEM analysis. HREM images (Fig. 5(a) and (b)) indicated that the covered layer is made of an agglomeration of nanostructures with the mean diameter of the crystallites to be 7 nm (±2 nm). The diffractogram of shell single crystal from HRTEM image (Fig. 5(c)) indicates rutile-type tin oxide (111) structure, which confirmed its polycrystalline nature and the presence of tin oxide (Fig. 5), which is known as a material with high chemical stability.[37,38] Moreover, STEM-EELS experiments of core/shell nanowire also confirmed the presence of SnO_2 shell (Fig. 6). In particular, SI-EELS performed on the area marked in green at Fig. 6(a) allow correlating HAADF signal with the elements distribution in the sample. HAADF signal is proportional to the element atomic number, therefore the difference on the HAADF contrast (Fig. 6(b)) suggests that the inner core has a different composition that the covered layer. Ag-$M_{4,5}$ (367 eV) and Sn-$M_{4,5}$ (485 eV) elemental maps (Fig. 6(c) and (d)) are extracted from the EELS raw data after removing the background using a power-law model and a window width of 25 eV maps. Silver atoms were evenly distributed along the nanowire core, while tin atoms were located in the outermost part of the nanowire (Fig. 6). The superimposition of the EELS maps for silver and tin showed the core/shell Ag/SnO_2 nanowire system.

To study the chemical state of the Ag/SnO_2NWs' surface, XPS analysis was used. Fig. S9(a)† presents the XPS survey spectrum for the Ag/SnO_2NWs sample characterised by high chemical stability indicating the presence of Sn, O, Ag, C and Au. Fig. S9 (b) and (c)† show respectively core level XPS Sn 3d and Ag 3d Ag/SnO_2NWs. The core level Sn 3d spectrum core/shell nanowires revealed the spin–orbit doublet at 487.1 eV (Sn $3d_{5/2}$) and 495.5 eV ($3d_{3/2}$) typical for Sn^{4+}, indicating the presence of SnO_2. The value of the Sn $3d_{5/2}$ and Sn $3d_{3/2}$ peak maxima are very close to the reported value for the SnO_2 surface,[39] confirming its high-quality crystal structure. The binding energy of the Ag $3d_{3/2}$ and Ag $3d_{5/2}$ peaks respectively at 373.9 and 367.9 eV indicated metallic silver (Ag^0) of nanowire core. Au is present in the XPS spectrum because Ag/SnO_2NWs were deposited on a silicon wafer coated with 100 nm of gold. Carbon (C 1s) comes from organic residues after the synthesis, such as citrate ions.

Recently, some reports have presented silver nanowires deposited on fabrics and their potential in wearable thermal management cloth. Ag nanoparticles anchored onto cellulose fibres formed high thermal insulating material characterized also by high breathability and antibacterial activity.[40] It was also shown that cellulose laminated on one side with carbon nanotubes can absorb sunlight and Ag-coated on the other side was used as an infrared reflector to minimize the human radiation heat output.[41] AgNWs/polydopamine composite attached to the

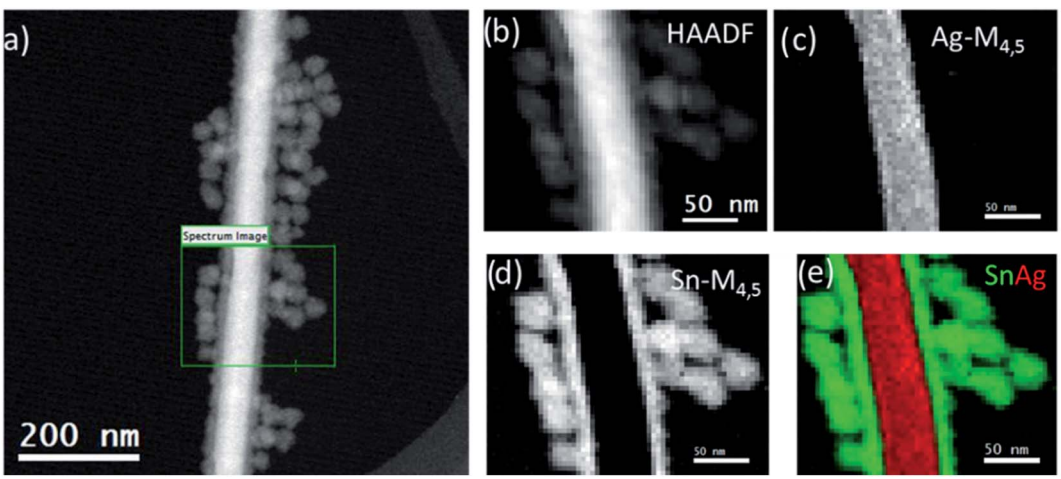

Fig. 6 (a) TEM and (b) high angular annular-dark-field (HADF) images and EELS map of (c) Ag-$M_{4,5}$, (d) Sn-$M_{4,5}$, and (e) EELS superimposed map of core/shell Ag/SnO_2NWs.

cotton fabric showed high IR reflectance, indicating higher thermal insulation capacity than unmodified fabric.[42] To reveal the impact of the SnO_2 shell on future Ag nanowire applications for designing smart wearable materials, the ability to reflect infrared radiation and reduce potential heat loss of the core/shell Ag/SnO_2 nanostructures was studied. The most atmospheric and liquid resistant hybrid was selected to the study to characterized infrared reflectance ability of the environmentally stable system. The SnO_2 coating obtained by a one-step hydrolysis process at 100 °C was selected as the most facile and effective method of AgNWs protection against harmful environmental influence. *Para*-Aramid fabrics were sprayed with aqueous solutions of the selected Ag/SnO_2NWs and AgNWs at the same concentration. *Para*-Aramid fabric without any coating acted as a control sample. The thermal diffusivity of pure *para*-aramid fabric was 1.05×10^{-7} ($\pm 1.7 \times 10^{-8}$) $m^2\ s^{-1}$. The thermal diffusivity of the coated fabrics was determined to be 1.77×10^{-7} ($\pm 1.9 \times 10^{-8}$) $m^2\ s^{-1}$ and 8.90×10^{-8} ($\pm 4.0 \times 10^{-9}$) $m^2\ s^{-1}$ with deposited AgNWs and Ag/SnO_2NWs, respectively. It indicated that AgNWs deposited on fabric only slightly change the heat transfer properties of the *para*-aramid. The core/shell Ag/SnO_2NWs decreased thermal diffusivity in the fabric by one order of magnitude due to the introduction of a semiconductor shell on the AgNWs surface.

To analyse the thermal properties of uncoated and nanowire coated *para*-aramid fabrics DSC studies were performed. Fig. 7(a) shows the thermograms for pure *para*-aramid fabric (control sample) and *para*-aramid fabric with deposited AgNWs and Ag/SnO_2NWs. DSC analysis of uncoated *para*-aramid fabric indicated its thermal decomposition in the temperature range of 526.0 to 590.4 °C and endothermic peak at about 580.8 °C (Fig. 7(a)), characteristic for aramid yarn.[43] The peak maximum was shifted to 572.5 °C and 579.8 °C for fabric coated with AgNWs and Ag/SnO_2NWs, respectively. The deposition of silver nanowires on fabric resulted in shifting the maximum of the endodermic peak to lower values by about 8 °C due to decreasing thermal degradation temperature. After fabric coating with SnO_2 shell, the maximum of the peak and the initial degradation temperature were shifted to the higher values by about 7 °C and 5 °C indicating the protective effect of the shell against the thermal decomposition process.

The degradation enthalpy value (ΔH_{deg}) for the uncoated *para*-aramid fabric was 269 J g^{-1} ΔH_{deg} for AgNWs and Ag/SnO_2NWs coated fabric was determined to be about 404 J g^{-1} and 320 J g^{-1}, respectively. The heat of thermal decomposition of the fabric with silver nanowires increased by about 50%. Ag/SnO_2NWs coated fabric revealed a decrease of thermal decomposition heat about 20% in comparison to AgNWs coated sample showing an increase of thermal stability of the sample after applying the SnO_2 layer on Ag nanostructure surface.

The thermogravimetric analysis revealed thermal decomposition of pure *para*-aramid fabric in the temperature range of 553.4 to 619.4 °C with the maximum peak at 584.8 °C (Fig. S10,† and 7(b)). The maximum of the peak shifted by 7.3 °C to the value of 577.7 °C after deposition of metallic nanostructures (AgNWs) on the fabric. Moreover, the end temperature for the process was lower about 20.8 °C indicating the lower temperature of fabric degradation. The initial temperature was noted at 561.3 °C and the process was finished at the temperature of 604.6 °C for fabric with deposited Ag/SnO_2NWs. The maximum of the peak was shifted to higher temperature values by 4.5 °C and the end temperature of the degradation process was shifted by 6 °C in comparison to the fabric coated with AgNWs. TG/DTG analysis confirmed the protective effect of SnO_2 shell on AgNWs and show an increase in their resistance to high temperatures. The mass loss for the samples was also calculated. The content of AgNWs and Ag/SnO_2NWs deposited on the *para*-aramid fabric was to be about 7.1 wt% and 15.2 wt%, respectively. Moreover, TG/DTG analysis of AgNWs and Ag/SnO_2NWs powders was carried out (Fig. S11†). TG thermogram for AgNWs showed the weight loss to be about 81.3 wt% in the temperature range of 401.2 to 458.1 °C connected with PVP thermal degradation. DTG thermogram showed the maximum peak at 228.5 °C, characteristic for PVP polymer.[20] PVP was used for AgNWs synthesis by polyol reduction method and acted as a capping agent, which further also stabilized silver colloid. The thermogram for Ag/SnO_2NWs powders did not reveal any mass loss in the studied temperature range indicating efficient SnO_2 shell formation. After Ag/SnO_2NWs hybrid formation PVP was

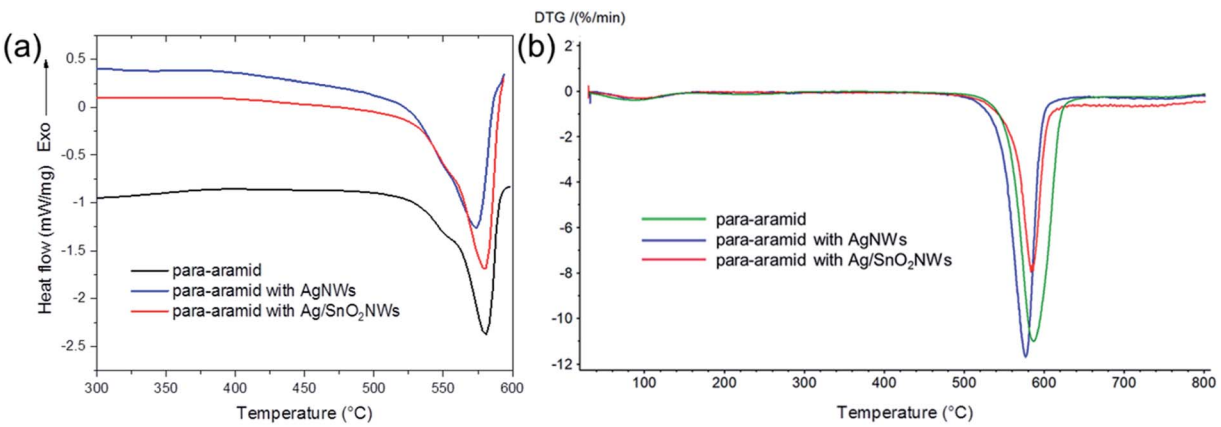

Fig. 7 (a) DSC and (b) DTG thermograms of *para*-aramid fabric with deposited Ag/SnO_2NWs, AgNWs and without nanowires (control sample).

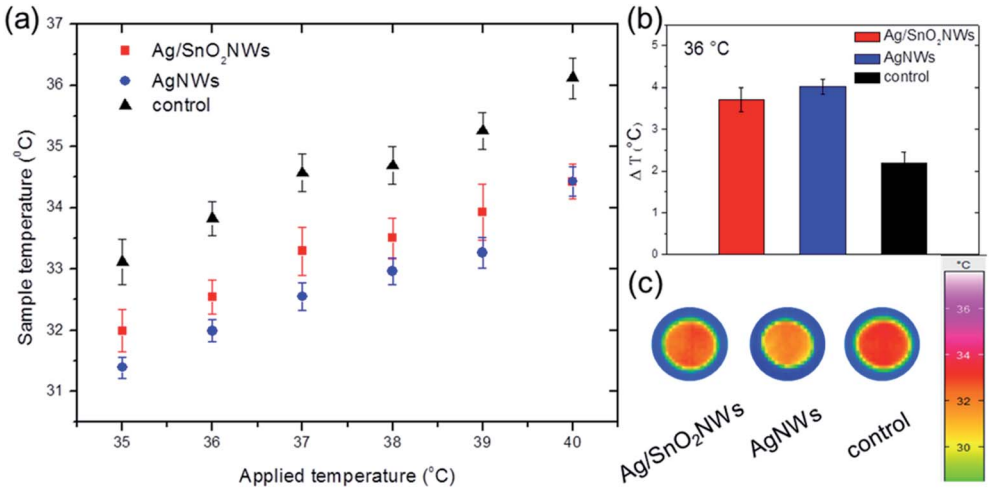

Fig. 8 (a) Sample temperature *vs.* applied temperature after placing the *para*-aramid fabric with deposited Ag/SnO_2NWs, AgNWs and without nanowires (control sample) on an open-air hot plate at 35 to 40 °C. (b) Heat transfer measurement by the temperature increase for an applied temperature of 36 °C. (c) Infrared images of the samples for an applied temperature of 36 °C.

removed by the filtration process and the colloid remained stable and homogenous. The shell protected AgNWs against aggregation without the addition of any surfactants.

Fig. 8 shows the comparison of the fabric surface temperature values after heating samples at different temperatures between 35 and 40 °C, in the range containing the temperature of the human body. The results show that pure *para*-aramid fabric has a minimal ability to reflect IR irradiation in comparison to the fabrics with the nanowires. The temperature differences between the fabrics with and without nanowires were significant, demonstrating efficient thermal insulation for the whole selected temperature range. Moreover, infrared radiation reflectivity for AgNWs was only slightly higher than for nanowires with the SnO_2 shell (Fig. S12,† and 8(b)), indicating that shell formation did not harm IR reflectance properties of AgNWs. The fabrics covered with AgNWs and Ag/SnO_2NWs had an 84% and 70% increase in temperature difference, respectively, indicating an effective thermal insulation effect for both coated samples (Fig. 8(b)). Fig. 8(c) shows infrared images of the samples for the applied temperature of 36 °C. IR images show that the temperatures of the fabrics covered with SnO_2 coated and uncoated silver nanowires are lower than that of the pure *para*-aramid fabric. Most of the thermal radiation of the sample with nanowires is reflected, while the pure fabric transferred the radiation effectively through the material, which is indicated by a dark red colour. The AgNWs provide more radiation insulation as a low-emissivity material[4] and retain these properties for silver nanowires coated with SnO_2, making the core/shell Ag/SnO_2 system useful for trapping the thermal radiation of the human body.

The results are consistent with other reports presenting silver-based thermal management, such as cotton coated with pure AgNWs,[4] AgNWs/cellulose films,[44] 3D silver platelets/reduced graphene oxide foam,[45] polyurethane sponges with Ag nanoparticles[46] or a combination of silver thin film and silica nanoparticles.[5] The heat transfer study of the samples with and without the SnO_2 shell, as well as the comparison to other studies, confirmed the core/shell Ag/SnO_2NWs as a good IR reflector. The core/shell nanostructures can be applied in designing fabrics for efficiently decreasing the heat loss from the human body in various conditions as a material characterized by high and long environmental stability.

Conclusions

In conclusion, we have presented the surface passivation technique of AgNWs by an SnO_2 shell through a one-step hydrolysis process of sodium stannate at 100 °C. The morphological, chemical, and structural characterisation of the core/shell Ag/SnO_2 nanowires revealed a 14 nm (±2 nm) thick SnO_2 shell consisting of 7 nm (±2 nm) rutile-type crystals surrounding the metallic core. The shell significantly influences the optical properties of the AgNWs. The plasmon responses in the longitudinal and transverse modes in the absorbance spectrum are red shifted from 349 and 376 nm to 361 and 415 nm, respectively, indicating that the AgNW's surrounding medium changes the dielectric constant. The SnO_2 shell significantly improves the atmospheric resistance of the AgNWs, which completely decompose after 9 weeks without a protective layer. The Ag/SnO_2NWs are stable for over 4 months at ambient conditions. The core/shell Ag/SnO_2NWs shows high liquid stability in the highly complexing environment of KCN. They are resistant to harsh CN^- ions at the concentration range of 0.01 to 0.0001 wt%. The absorbance intensity spectrum of the Ag/SnO_2NWs only slightly decreases for 0.1 wt% cyanide ion concentration.

The report also presents microwave assisted SnO_2 shell formation at 100 °C and microwave irradiated Ag/SnO_2NWs after the shell synthesis. The microwave treatment is a commonly used technique for synthesis and improving the crystal structure of various semiconductor coatings. This study shows that a simple hydrolysis process at 100 °C is a facile,

effective method to obtain a protective coating on AgNWs. The microwave irradiation allows core/shell Ag/SnO_2 nanostructures to be obtained, however they do not show long-term stability in both atmospheric conditions and KCN solution. Moreover, the shell formation under microwave treatment is not fast enough to inhibit the early start of the AgNWs decomposition process, and the formation of silver prismatic triangular shaped structures. The Ag/SnO_2NWs, microwave treated after the shell synthesis, also show low environmental stability, they decompose after 5 weeks under ambient conditions.

The selected Ag/SnO_2NWs obtained at 100 °C in aqueous solution revealed high atmospheric and chemical stability. This most stable core/shell Ag/SnO_2NWs composite and pure AgNWs were deposited on *para*-aramid fabric. DSC analysis shows that the maximum of the degradation peak and the initial degradation temperature for the fabrics with Ag/SnO_2NWs are shifted to the higher values by about 7 °C and 5 °C in comparison to AgNWs coated fabric indicating the protective effect of the shell against the thermal decomposition process.

TG/DTG analysis confirms the protective effect of the SnO_2 shell on AgNWs and shows an increase in their resistance to high temperatures on *para*-aramid fabric. The maximum of the DTG peak is shifted to higher temperature values by 4.5 °C in comparison to the fabric coated with AgNWs. The Ag/SnO_2NWs decreases also thermal diffusivity of the fabric by one order of magnitude due to the introduction of a semiconductor shell on the AgNWs surface.

Moreover, the *para*-aramid fabric, after covering it with Ag/SnO_2NWs, shows a significant increase in the IR reflection efficiency, which is comparable to pure AgNWs. It reveals that SnO_2 shell synthesis does not affected significantly IR reflectivity of Ag core. Our findings indicate that core/shell Ag/SnO_2-NWs represents a very promising material, characterised by high IR reflection as well as high environmental stability, for the fabrication of effective wearable "personal thermal management" devices in the near future.

Conflicts of interest

There are no conflicts to declare.

Acknowledgements

The research was financially supported by a grant from the National Science Centre, Poland (Opus 15 no. 2018/29/B/ST8/02016). The authors would like to thank Dr Paweł Swaczyna (ŁUKASIEWICZ–Textile Research Institute, Department of Mechanical Textiles Technologies) for his technical contribution in the infrared thermography studies, Dr Katarzyna Śledzińska (ŁUKASIEWICZ–Textile Research Institute, Department of Mechanical Textiles Technologies) for the measurements of thermal conductivity and Dr Zbigniew Malinowski (Department of Organic Chemistry, University of Lodz, Poland) for making the Microwave Reaction System device available and assistance with measurements. We are grateful for the assistance of Dr Jan Čechal and the opportunity to use the XPS of the Central European Institute of Technology (CEITEC) Nano Research Infrastructure (Brno, the Czech Republic). HRTEM and STEM-EELS studies were performed at the DME Facilities of SCCYT of the University of Cádiz.

References

1 W. Li, H. Zhang, S. Shi, J. Xu, X. Qin, Q. He, K. Yang, W. Dai, G. Liu, Q. Zhou, H. Yu, S. R. P. Silva and M. Fahlman, *J. Mater. Chem. C*, 2020, **8**, 4636–4676.
2 J. Li and F. Leonard Deepak, *Chem. Commun.*, 2020, **56**, 4765–4768.
3 Y. Lian, H. Yu, M. Wang, X. Yang, Z. Li, F. Yang, Y. Wang, H. Tai, Y. Liao, J. Wu, X. Wang, Y. Jiang and G. Tao, *J. Mater. Chem. C*, 2020, **8**, 8399–8409.
4 P. C. Hsu, X. Liu, C. Liu, X. Xie, H. R. Lee, A. J. Welch, T. Zhao and Y. Cui, *Nano Lett.*, 2015, **15**, 365–371.
5 Q. Liu, J. Huang, J. Zhang, Y. Hong, Y. Wan, Q. Wang, M. Gong, Z. Wu and C. F. Guo, *ACS Appl. Mater. Interfaces*, 2018, **10**, 2026–2032.
6 H. J. Hwang, H. Devaraj, C. Yang, Z. Gao, C. hung Chang, H. Lee and R. Malhotra, *Sci. Rep.*, 2018, **8**, 1–12.
7 A. Khan, V. H. Nguyen, D. Muñoz-Rojas, S. Aghazadehchors, C. Jiménez, N. D. Nguyen and D. Bellet, *ACS Appl. Mater. Interfaces*, 2018, **10**, 19208–19217.
8 J. L. Elechiguerra, L. Larios-Lopez, C. Liu, D. Garcia-Gutierrez, A. Camacho-Bragado and M. J. Yacaman, *Chem. Mater.*, 2005, **17**, 6042–6052.
9 Y. Zhang, J. Xia, J. Xu, B. Sun, W. Wu and L. Zhu, *Environ. Sci.: Nano*, 2018, **5**, 2452–2460.
10 T. C. Kaspar, T. Droubay, S. A. Chambers and P. S. Bagus, *J. Phys. Chem. C*, 2010, **114**, 21562–21571.
11 Y. Yang, Q. Zhang, Z. W. Fu and D. Qin, *ACS Appl. Mater. Interfaces*, 2014, **6**, 3750–3757.
12 P. Ramasamy, D. M. Seo, S. H. Kim and J. Kim, *J. Mater. Chem.*, 2012, **22**, 11651–11657.
13 A. Baranowska-Korczyc, K. Sobczak, P. Dłużewski, A. Reszka, B. J. Kowalski, Ł. Kłopotowski, D. Elbaum and K. Fronc, *Phys. Chem. Chem. Phys.*, 2015, **17**, 24029–24037.
14 H. W. Kim, H. G. Na, Y. J. Kwon, S. Y. Kang, M. S. Choi, J. H. Bang, P. Wu and S. S. Kim, *ACS Appl. Mater. Interfaces*, 2017, **9**, 31667–31682.
15 A. Debataraja, D. W. Zulhendri, B. Yuliarto, Nugraha, Hiskia and B. Sunendar, *Procedia Eng.*, 2017, **170**, 60–64.
16 A. Baranowska-Korczyc, E. Mackiewicz, K. Ranoszek-Soliwoda, J. Grobelny and G. Celichowski, *RSC Adv.*, 2020, **10**, 38424–38436.
17 B. Bob, A. Machness, T. Bin Song, H. Zhou, C. H. Chung and Y. Yang, *Nano Res.*, 2016, **9**, 392–400.
18 Y. Zhao, X. Wang, S. Yang, E. Kuttner, A. A. Taylor, R. Salemmilani, X. Liu, M. Moskovits, B. Wu, A. Dehestani, J. F. Li, M. F. Chisholm, Z. Q. Tian, F. R. Fan, J. Jiang and G. D. Stucky, *J. Am. Chem. Soc.*, 2019, **141**, 13977–13986.
19 M. Cieślak, E. Gromadzińska, I. Kamińska, E. Witczak and K. Śledzińska, *Text. Res. J.*, DOI: 10.1177/0040517520970170.
20 P. Giesz, E. Mackiewicz, A. Nejman, G. Celichowski and M. Cieślak, *Cellulose*, 2017, **24**, 409–422.

21 P. Giesz, E. Mackiewicz, J. Grobelny, G. Celichowski and M. Cieślak, *Carbohydr. Polym.*, 2017, **177**, 397–405.
22 H. E. Bennett, R. L. Peck, D. K. Burge and J. M. Bennett, *J. Appl. Phys.*, 1969, **40**, 3351–3360.
23 J. P. Franey, G. W. Kammlott and T. E. Graedel, *Corros. Sci.*, 1985, **25**, 133–143.
24 T. E. Graedel, *J. Electrochem. Soc.*, 1992, **139**, 1963.
25 S. Phadungdhitidhada, P. Ruankham, A. Gardchareon, D. Wongratanaphisan and S. Choopun, *Adv. Nat. Sci.: Nanosci. Nanotechnol.*, 2017, **8**, 035004.
26 M. Abulikemu, M. Neophytou, J. M. Barbé, M. L. Tietze, A. El Labban, D. H. Anjum, A. Amassian, I. McCulloch and S. Del Gobbo, *J. Mater. Chem. A*, 2017, **5**, 7759–7763.
27 M. T. X. Nguyen, H. K. P. Huynh, H. Q. Dang, H. T. Nguyen, C. T. Le, Y. N. Pham, T. H. Luu and S. T. Nguyen, *Chem. Eng. Trans.*, 2020, **78**, 169–174.
28 Y. Gao, P. Jiang, L. Song, L. Liu, X. Yan, Z. Zhou, D. Liu, J. Wang, H. Yuan, Z. Zhang, X. Zhao, X. Dou, W. Zhou, G. Wang and S. Xie, *J. Phys. D: Appl. Phys.*, 2005, **38**, 1061–1067.
29 S. Fahad, H. Yu, L. Wang, Y. Wang, T. Elshaarani, B. U. Amin, K. U. R. Naveed, R. U. Khan, S. Mehmood, F. Haq, Z. Ni and M. Usman, *CrystEngComm*, 2020, **22**, 2183–2196.
30 Tanvi, A. Mahajan, R. K. Bedi, S. Kumar, V. Saxena, A. Singh and D. K. Aswal, *RSC Adv.*, 2016, **6**, 48064–48071.
31 A. Amirjani, N. N. Koochak and D. F. Haghshenas, *J. Chem. Educ.*, 2019, **96**, 2584–2589.
32 H. I. Sang, T. L. Yun, B. Wiley and Y. Xia, *Angew. Chem., Int. Ed.*, 2005, **44**, 2154–2157.
33 M. A. Mahmoud, M. Chamanzar, A. Adibi and M. A. El-Sayed, *J. Am. Chem. Soc.*, 2012, **134**, 6434–6442.
34 L. Shang, C. Qin, L. Jin, L. Wang and S. Dong, *Analyst*, 2009, **134**, 1477–1482.
35 S. Hajizadeh, K. Farhadi, M. Forough and R. E. Sabzi, *Anal. Methods*, 2011, **3**, 2599–2603.
36 P. Giesz, G. Celichowski, D. Puchowicz, I. Kamińska, J. Grobelny, D. Batory and M. Cieślak, *Cellulose*, 2016, **23**, 2143–2159.
37 J. Gong, X. Wang, X. Fan, R. Dai, Z. Wang, Z. Zhang and Z. Ding, *Opt. Mater. Express*, 2019, **9**, 3691.
38 V. B. Kamble and A. M. Umarji, *Sens. Actuators, B*, 2016, **236**, 208–217.
39 Y. N. N. Ikeo, Y. Iijima, N. Nimura, M. Sigematsu, T. Tazawa, S. Matsumoto and K. Kojima, *Handbook of X-ray Photoelectron Spectroscopy*, Jeol, 1991.
40 X. Yue, T. Zhang, D. Yang, F. Qiu, Z. Li, G. Wei and Y. Qiao, *J. Colloid Interface Sci.*, 2019, **535**, 363–370.
41 X. Yue, M. He, T. Zhang, D. Yang and F. Qiu, *ACS Appl. Mater. Interfaces*, 2020, **12**, 12285–12293.
42 Z. Yu, Y. Gao, X. Di and H. Luo, *RSC Adv.*, 2016, **6**, 67771–67777.
43 A. Nejman, I. Kamińska, I. Jasińska, G. Celichowski and M. Cieślak, *Molecules*, 2020, **25**, 11–13.
44 C. Liang, K. Ruan, Y. Zhang and J. Gu, *ACS Appl. Mater. Interfaces*, 2020, **12**, 18023–118031.
45 C. Liang, P. Song, H. Qiu, Y. Zhang, X. Ma, F. Qi, H. Gu, J. Kong, D. Cao and J. Gu, *Nanoscale*, 2019, **11**, 22590.
46 C. Liang, Y. Liu, Y. Ruan, H. Qiu, P. Song, J. Kong, H. Zhang and J. Gu, *Composites, Part A*, 2020, **139**, 106143.